LA-UR -88-797

CONF-880564--14

Los Alamos National Laboratory is operated by the University of California for the United States Department of Energy under contract W-7405-ENG-36

LA-UR--88-797

DE88 007899

TITLE TIME-RESOLVED DOUBLY BENT CRYSTAL X-RAY SPECTROMETER

AUTHOR(S) M. P. Hockaday, R. L. Blake, J. Vaninetti, P-14
M. D. Wilke, N. T. Gray, P-15
P. T. Nedrow, EG&G/LAO

SUBMITTED TO Proceedings of the Topical Conference on High Temperature Plasma Diagnostics, March 13-17, 1988, Napa, CA

DISCLAIMER

MASTER

Los Alamos Los Alamos National Laboratory
Los Alamos, New Mexico 87545

TIME-RESOLVED DOUBLY BENT CRYSTAL X-RAY SPECTROMETER*

M. P. Hockaday, M. D. Wilke, R. L. Blake, J. Vaninetti, N. T. Gray

Physics Division, Los Alamos National Laboratory

P. O. Box 1663, MS D410

Los Alamos, New Mexico 87545

P. T. Nedrow

EG&G Energy Measurements, Inc, Los Alamos Operations

P. O. Box 809

Los Alamos, New Mexico 87544

ABSTRACT

X-ray spectroscopy is an essential tool in high temperature plasma research. We describe a time-resolved x-ray spectrometer suitable for measuring spectra in harsh environments common to many very high energy density laboratory plasma sources. The spectrometer consisted of a doubly curved Si(111) crystal diffraction element, a WL-1201 (ZnO:Ga) phosphor, a coherent fiber optic array, and two visible streak cameras. The spectrometer design described here has a minimum time resolution of 1.3 ns with 2.8 eV spectral resolution over a 200 eV wide bandpass in the 6-7 keV region of the spectrum. Complete system spectral throughput calibrations were done at the Cornell High Energy Synchrotron (CHESS). Details of the design and calibration results are presented.

* Work performed under the auspices of USDOE.

INTRODUCTION

High resolution spectroscopy can be used to determine many physical parameters in high temperature plasmas. By observing the spectra as a function of time one can follow the physical evolution of the plasma. The energy resolution of a crystal spectrometer is determined by the inherent energy width of the crystal's Bragg diffraction pattern and the effective energy width of the spectrometer's slit system. To limit the overall effect of the slit system on the energy resolution, it is necessary to make the subtended angular slit width from the crystal small. The energy resolution is also controlled by the number of resolvable elements of the detector system. The time resolution of the system is the convolution of the time response of all the components of the detection system. In the case of the spectrometer described here, the total time resolution is given by the convolution of the phosphor time response, the dispersion effects of the fiber, and the inherent time response of the streak camera itself. Proper choices in the phosphor and fiber optics used in such a system can minimize the system time response. To the best of our knowledge the crystal geometry described in this paper is the first implementation of a doubly curved elliptical geometry.

I. INSTRUMENT

A. Crystal

The silicon (111) atomic planes ($2d = 6.2712$ Å) were chosen for this application because the theoretical width of the x-ray diffraction pattern at 6.65 keV is 0.82 eV (based on the general dynamical theory of diffraction[1]),

near-perfect crystal specimens are readily available, and because silicon was thought to be adequately flexible in thin sections.

The 3.5 cm by 3.5 cm crystal was thinned to 226 μm and etched to relieve stress. One side was then polished flat parallel to the Si(111) planes and parallel to the opposite side. The polished side of the crystal was epoxied to a machined aluminum mandrel. The mandrel's curvature was elliptical[2] in the dispersion direction and had a changing cylindrical radius of curvature in the perpendicular direction. The crystal, mandrel, and slit geometry are depicted in Fig. 1. The elliptical geometry allowed for the use of a scatter slit at the second focus, and a narrow slit at the first focus (spectrometer input), to improve the purity and energy resolution of the system, respectively. The cylindrical radius was varied from the low energy end to the high energy end of the crystal such that all energies were in vertical focus along a linear fiber array placed perpendicular to the central spectral ray. This cylindrical curvature increases the flux at the detector plane. The exact cylindrical curvature, r_C, was determined by the dimensions of the spectrometer and the height of the fiber array according to the equations:

$$r_C = (\rho + R_D)\sin\beta(R_O/L)$$

and

$$\beta = \theta + \cos^{-1}(\cos\theta/\epsilon).$$

Where θ is the Bragg angle of the wavelength of interest, ρ is the distance from the corresponding location on the crystal to the second focus, R_D is the distance from the location on the crystal to the corresponding detector

location, R_0 is the distance between foci, L is the distance from the first foci to the detector location, and ϵ is the eccentricity of the ellipse.

B. Phosphor and Fiber Optic Array

The phosphor WL-1201(ZnO:Ga) was chosen because of its relatively fast response of 800 ps and its high conversion efficiency of x-rays to 400 nm light.

We used two stacked linear coherent fiber arrays to take a 200 eV bite out of the spectrum with each stacked fiber pair width corresponding to 1 eV in the dispersion plane (see Fig. 2). The two arrays increased the dynamic range of the system for single shot experiments by allowing the use of two streak cameras with different gain settings. To insure that each row of fibers observed identical signals, a rectangular parallelopiped coupling scheme[4] depicted in Fig. 2 was used. Two rows of 200 fibers were stacked one on top of the other. A set of 140 μm by 280 μm by 3 mm UV transmitting glass parallelopipeds was coupled to the front of the array such that a vertical pair of fibers were coupled to each rod. These rectangular rods act like mixers because light from a lambertian source which enters at any point on the entrance face exits nearly uniformly on the exit face. Any nonuniformities in the focal plane are smoothed and the two streak cameras will receive the same signal. On the other end of the fiber bundle, each row of fibers is built into a separate array head and directly coupled to a streak camera. The fiber arrays were built at EG&G, Atlas and the glass mixers were assembled by EG&G, Santa Barbara.

The fiber optic array was made of 35 m long Polymicro 100μm/110μm/135μm (core/cladding/jacket) fibers. The array length provides

optical delay long enough for the streak camera to be triggered from a separate detector viewing the source and allows remote location of the streak camera in a protective screen room away from any electromagnetic pulse (EMP) of the source.

The two row fiber array was only 280 μm high, making alignment critical in order to intercept the ~1 mm high focused image of the source slit. Alignment changes in the position of the slit with respect to the spectrometer over time, caused by building motion or thermal gradients along the line of sight, are corrected by motor translation of the array, based on the pre-aligned position of an intensified CID camera image of an alignment slit shown in Fig. 1.

C. Streak Camera and TV Readout

The two visible streak cameras each consisted of a RTC Phillips Model 501 streak tube coupled to an ITT model 4113 microchannel plate (MCP) intensifier. A Xedar Model 503A fast scan TV camera[5] equipped with a 88XQ 28 mm PbO target vidicon was used as a readout system. Data were recorded on LeCroy 8857, 50 MHz, 8-bit digitizers. The use of the TV camera and digitizers allowed direct storage onto a computer without having to develop film and subsequently digitize the film with the use of a densitometer. It is important to calibrate the streak cameras, TV readout, and the digitizer as a system to obtain high accuracy from experimental measurements.

II. Calibration

A. Piecemeal

Several different flat Si(111) crystals' diffraction characteristics were measured at the Fe K_α x-ray energy and at several locations across their surfaces. The final samples that were chosen for mounting had a variation in the diffraction pattern FWHM of 3% across the surfaces of the crystals. The focussing properties of the mounted crystals were investigated. The focussed image at the detector was approximately 1 mm high and contained structure due to imperfections in the crystal - mandrel combination. Our experience showed that even crystals thinned to 250 μm have large scale stress distortions when bent to radii of curvature ~10 cm.

The time response of the WL-1201 phosphor was measured to be 800 ps using the 6 MeV, 50 ps FWHM electron Linac at EG&G, Santa Barbara. In addition, the wavelength dispersion characteristics and the attenuation of the Polymicro fiber at 400 nm were measured at EG&G, SBO and found to be 1.3 ps/nm and 0.06 dB/m, respectively. The resultant temporal response of the phosphor light (18 nm FWHM) through the fiber was 1.13 ns.

The conversion efficiency of x-rays to light as a function of wavelength and thickness was measured at CHESS between 5 and 20 keV.[3] The conversion efficiency was measured to be ~0.01 W(visible)/W(x ray) at 6.7 keV.

The streak camera and readout system voltage as a function of 400 nm light intensity and gain setting were taken for both cameras. Background and uniform field calibrations were also taken. A 500 MHz rate, 150 ps FWHM, pulsed laser diode provided the sweep speed calibration. The time resolution

of the streak camera for a 90 ns sweep was 600 ps. The total system temporal response was then 1.3 ns FWHM.

B. System

The spectrometer was taken to CHESS for a full system calibration using the C2 beamline. A schematic of the calibration measurement is shown in Fig. 3. For the calibration run, the horizontal electron bunch width of the synchrotron beam was used to define the source size at the elliptical first focus. Nitrogen ion chambers were used to measure the absolute throughput of the spectrometer. The spectrometer was evacuated with a roughing pump. Only the p-polarization efficiency was measured; however, at the Bragg angles that we used there is a negligible difference in p and σ reflectivities of the crystals. Due to the vertical collimation of the x-ray beam, only an approximately 100 eV wide band satisfied the Bragg condition at any one setting of the spectrometer. A typical plot of the measured efficiency of the curved crystal is shown in Fig. 5. The indicated fall off is due to the geometry of the system and not the efficiency of the crystal. The phoshor-fiber array was placed at the spectrometer focus and the signals were recorded by the streak camera system. Because of the low intensity of the synchrotron beam, it was necessary to run the streak camera in the ungated, unswept (DC) mode. In the DC mode, an average of 2.18×10^3 synchrotron x-ray pulses of 150 ps width were integrated over the 8 ms field time of the readout. The two crystal CHESS monochromator provided a ~1 eV wide input to the spectrometer. The resultant DC system response at a variety of energies between 6.5 and 6.8 keV was measured. A typical system response calibration is shown in Fig.

6. The FWHM of the measured curve is 2.00 eV; therefore, the initial 1 eV resolution input signal was smeared into a 2.00 eV wide equivalent system point spread function on the streak camera. The average equivalent system point spread function over the 200 eV bandpass was 2.75 eV wide.

SUMMARY

The characteristics of a doubly curved, time-resolved crystal x-ray spectrometer system were measured to give the designed 200 eV bandpass with 2.75 eV spectral resolution and 1.3 ns temporal resolution near 6.6 keV for a time interval ≤90 ns. A dynamic range of greater than 10^3 was possible with the choice of the streak camera and fiber optic system. This type of spectrometer has applications to many high temperature plasmas, such as plasma focus, ICF laser, Z-pinch, and some magnetic confinement fusion sources.

ACKNOWLEDGEMENTS

We thank Steve Iversen, Charles Iversen, Dante Berry, Evan Ballard, Rodger Liljestrand, and Doug Fulton for their efforts in the design, construction, and calibration of the spectrometer described here. We are also grateful to the staff and operators at CHESS for advice, support and beam time.

REFERENCES

[1]B. W. Batterman, and H. Cole, Rev. Mod. Phys. **36**, 681 (1964).

[2]B. L. Henke, H. T. Yamada, and T. J. Tanaka, Rev. Sci. Instrum. **54**, 1311 (1983).

[3]M. D. Wilke, R. L. Blake, S. Iverson, K. Moy, M. P. Hockaday, N.King, and R. .H. Day, "Synchrotron Measurements of the X-Ray Response of Fast Phosphors," to be published.

[4]EG&G Energy Measurements Group, Santa Barbara, California, report EGG 10282-2163 (1987).

[5]B.W. Noel, and G. J. Yates, Rev. Sci. Instrum. **53**, 1764 (1982).

Fig. 1. A schematic of the spectrometer configuration. The spectrometer input slit is at the first focus of the elliptical curvature in the direction of dispersion. A cylindrical curvature provides line-focusing of the input slit image at the detector plane. A phosphor-fiber optic array is mounted at the detector location.

Fig. 2. The phosphor-fiber optic array coupling scheme. Two sets of 200 fibers were stacked on top of each other and coupled to UV glass parallelopipeds as shown.

Fig. 3. Calibration geometry at CHESS. The monochromator was used to scan the energies between 6.6 and 6.8 keV.

Fig. 4. Efficiency as a function of energy of the crystal at one setting of the spectrometer. Efficiency has been adjusted to account for the area of the beam that is incident at the proper Bragg angle.

Fig. 5. DC recorded data from a LeCroy digitizer. The input into the spectrometer was a 1 eV wide beam at 6.65 keV. The resultant recorded width is 2.00 eV.

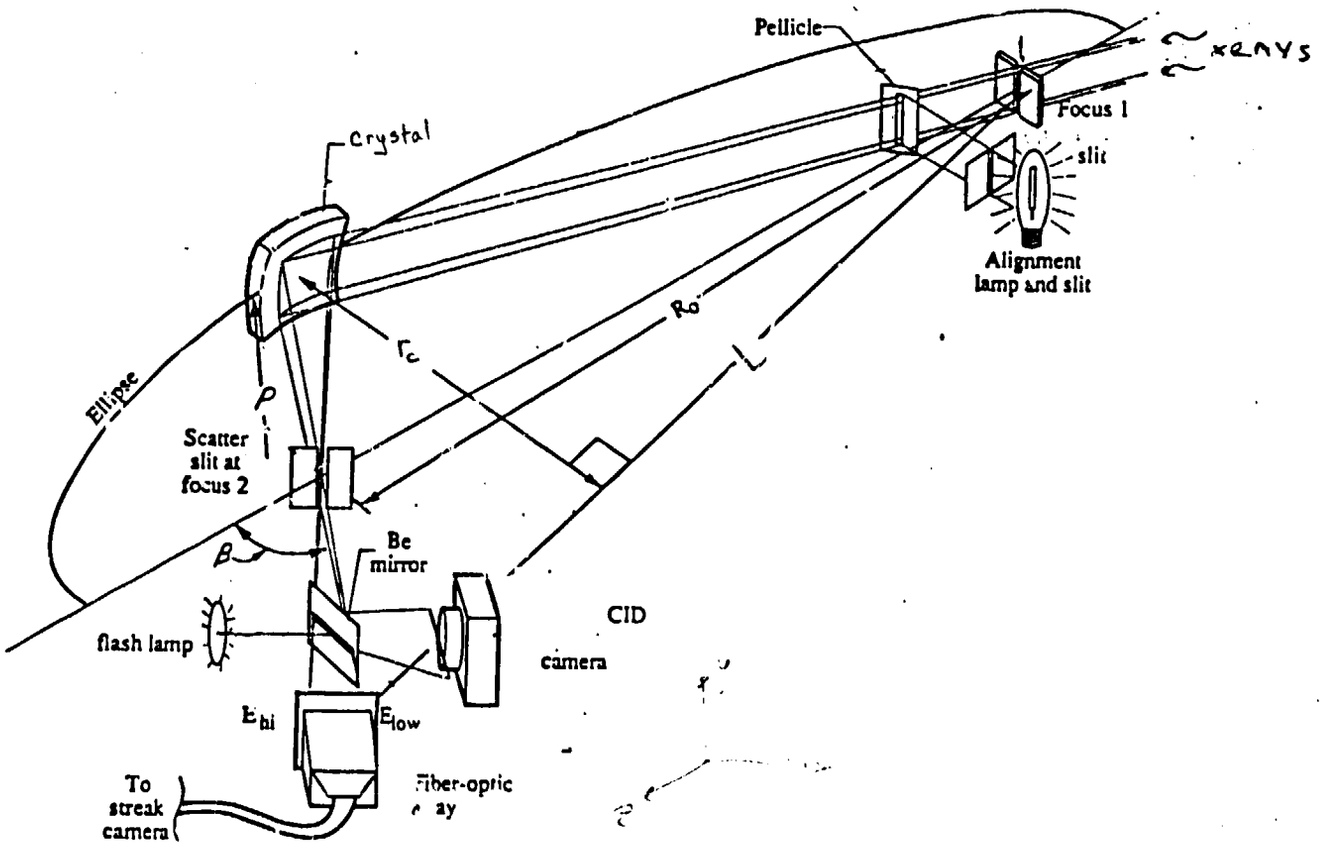
Pellicle
~ x-rays
Focus 1
slit
Alignment lamp and slit
Crystal
Ro
rc
L
ρ
Ellipse
Scatter slit at focus 2
β
Be mirror
CID
camera
flash lamp
Ehi
Elow
To streak camera
Fiber-optic

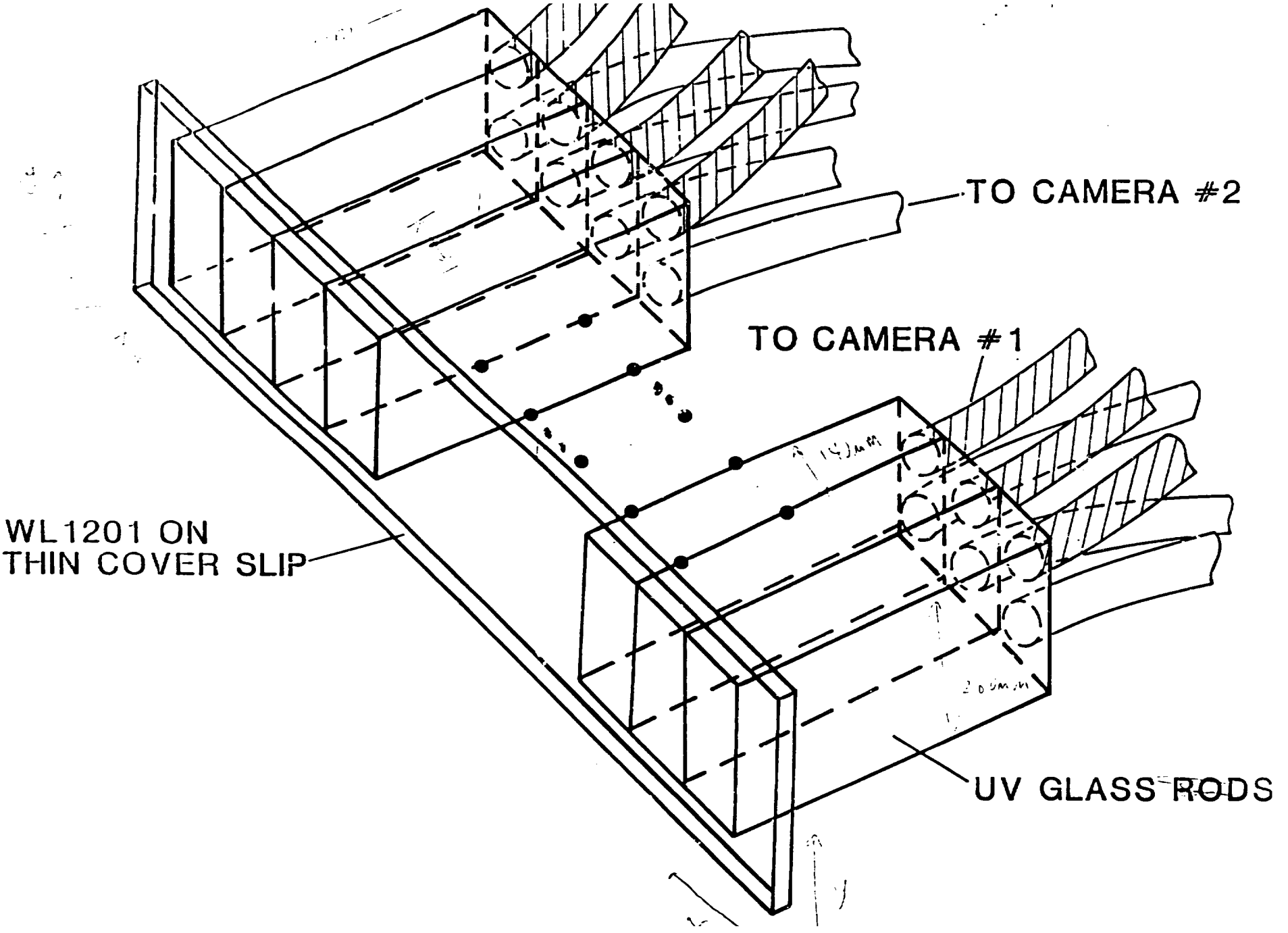
TO CAMERA #2
TO CAMERA #1
WL1201 ON
THIN COVER SLIP
UV GLASS RODS

SYNCHROTRON CALIBRATION GEOMETRY

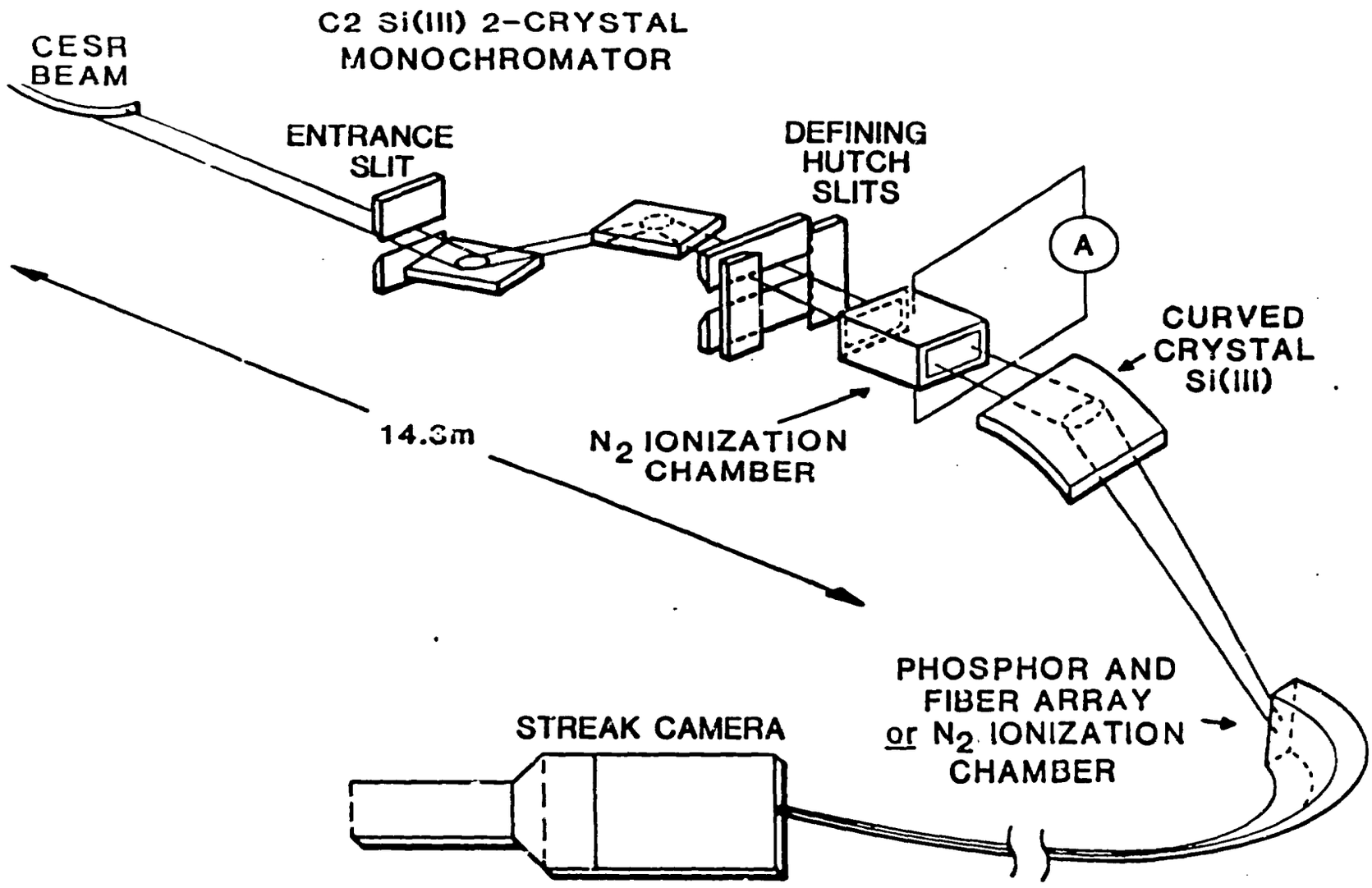

Fig 3

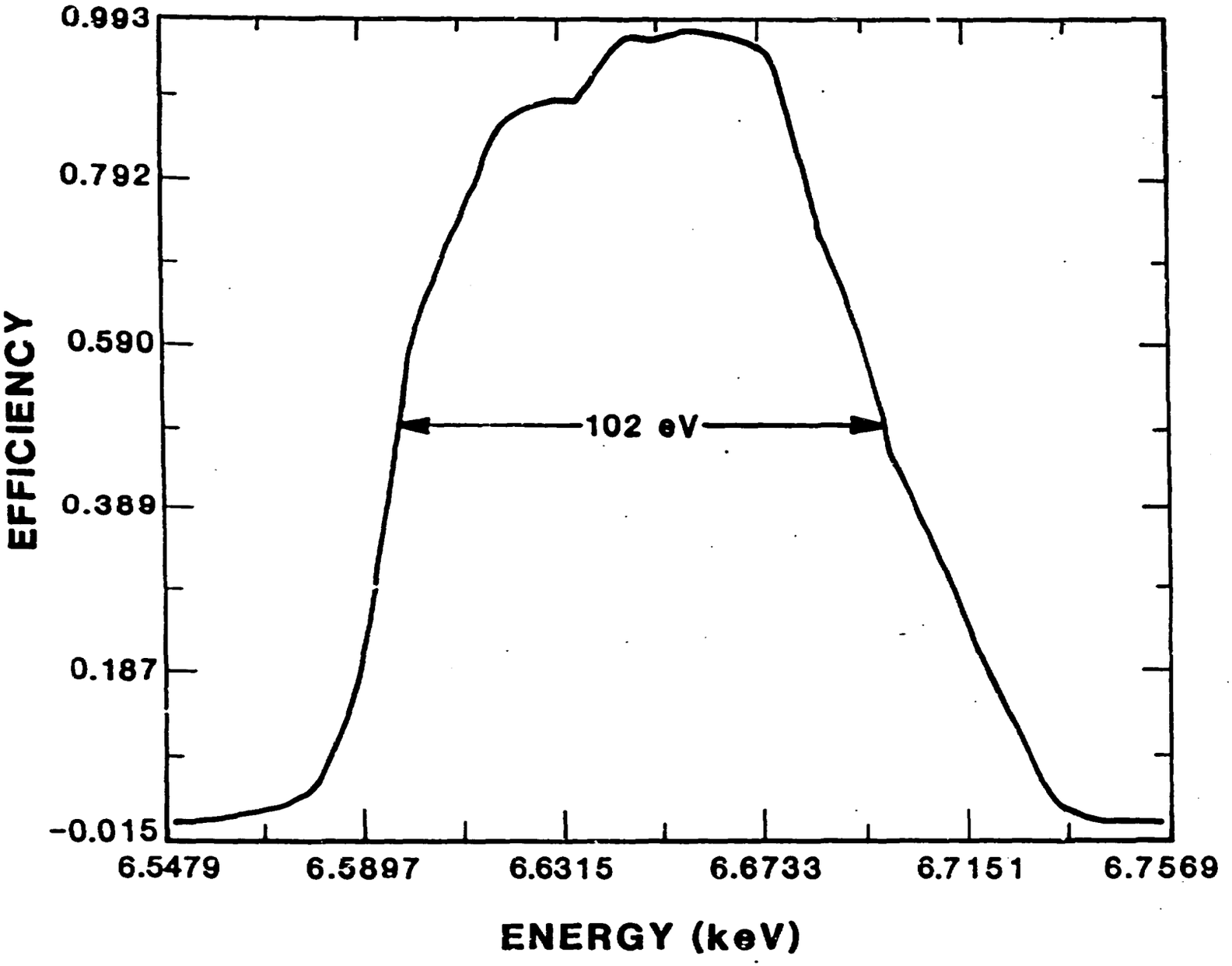
0.993
0.792
0.590
0.389
0.187
-0.015
EFFICIENCY
102 eV
6.5479
6.5897
6.6315
6.6733
6.7151
6.7569
ENERGY (keV)

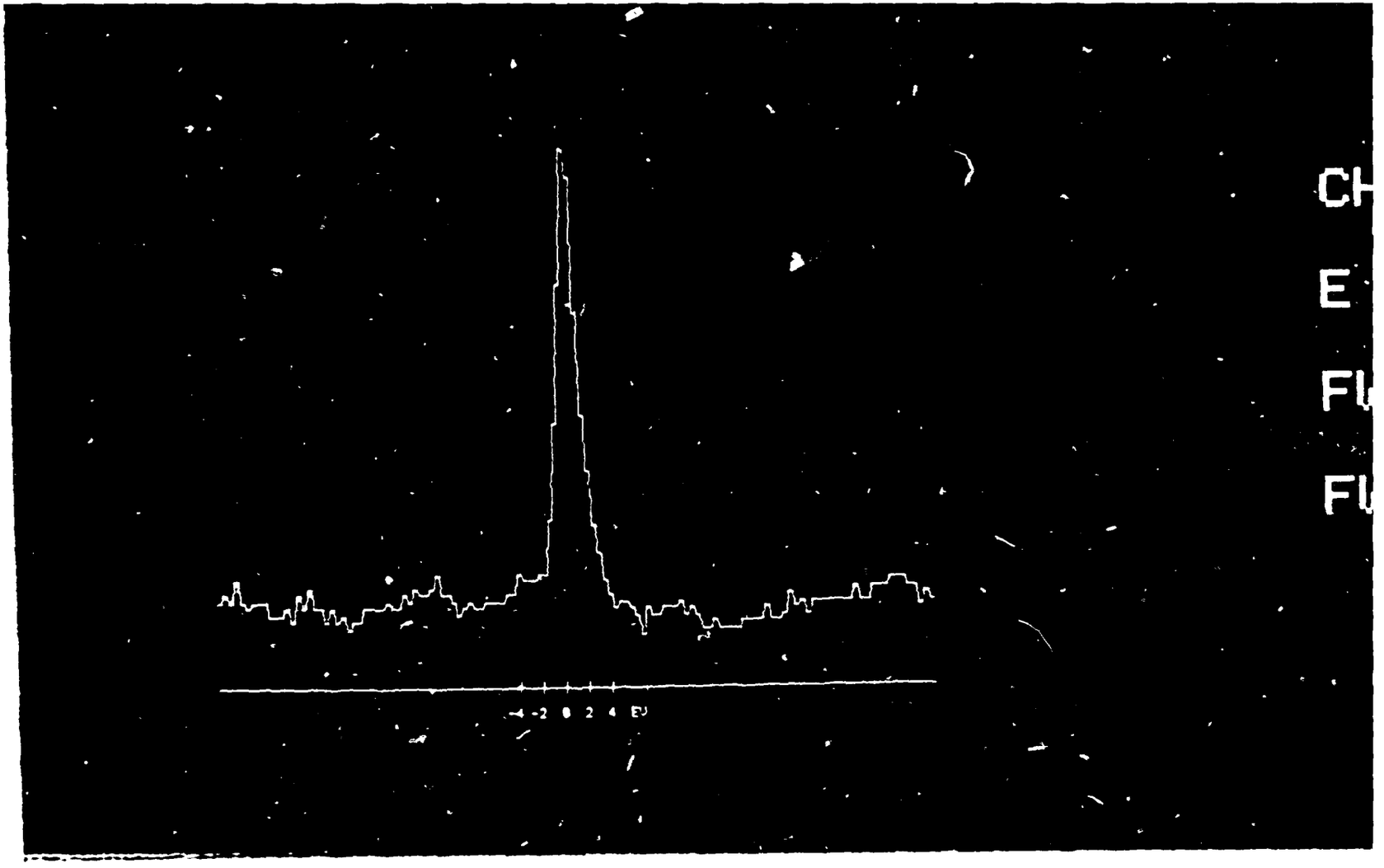
-4 -2 0 2 4 EV